Biomed Microdevices (2013) 15:531–537
DOI 10.1007/s10544-013-9752-1

Shadow masking for nanomaterial-based biosensors incorporated with a microfluidic device

Jiyong Huang · Innam Lee · Xiliang Luo · Xinyan Tracy Cui · Minhee Yun

Published online: 19 February 2013

Abstract Integrating PDMS channels and chips containing pre-functionalized biosensors into microfluidic devices with irreversible sealing has been challenging because the integration process requires use of an O_2 plasma treatment that usually destroys the biosensors. In this study, we examined the usefulness of introducing a shadow mask into the process as a method of protecting the pre-functionalized biosensors. Single nanowire sensors were pre-functionalized with fluorescently labeled biomolecules and then subjected to O_2 plasma with and without the shadow mask. Results from the two groups were then compared. Those sensors without a shadow mask were destroyed, giving the sensor an infinite resistance and reduced fluorescence intensity. In contrast, the sensors with the shadow mask were protected and exhibited little changes in the resistance and fluorescence intensity. Then two different nanowires, aptamers incorporated polypyrrole nanowire (entrapment) and antibodies immobilized polyaniline nanowire (surface covalent binding), were used to investigate their detection performance before and after the plasma treatment in the presence of shadow mask. The protected samples showed a good sensitivity to the targets with a slight reduction in response compared with the as-prepared samples. After the O_2 plasma treatment, the microfluidic channels were integrated with single nanowire biosensors. This microfluidic biosensor showed a high sensitivity with about ~0.5 % change in conductance at the lowest IgE protein concentration of 10 pM.

J. Huang · I. Lee · M. Yun (✉)
Department of Electrical and Computer Engineering, University of Pittsburgh, Pittsburgh, PA 15261, USA
e-mail: miy16@pitt.edu

X. Luo · X. T. Cui
Department of Bioengineering, University of Pittsburgh, Pittsburgh, PA 15261, USA

Keywords Shadow mask · Microfluidics · Biosensors · Nanowires · Conducting polymers

1 Introduction

Microfluidic devices are of considerable interest for use in biosensors because of several advantages that they provide, including reduced consumption of sample, protection of the sensor by the microchannels from the environment, and comparatively fast and more sensitive reactions (Kwakye and Baeumner 2003). Consequently, microfluidic devices have been used in various areas, such as biological and chemical analysis (Liu et al. 2005), point-of-care testing (Soper et al. 2006), clinical analysis (Bange et al. 2005), and medical diagnosis (Goral et al. 2006). Numerous applications found in the current literature include the detection of pathogens (Zaytseva et al. 2005), the quantification of nucleic acid sequences (Goral et al. 2006), and analysis of multiple ions (Liao et al. 2006). While most microfluidic biosensors use fluorescence (Chan et al. 2004; Liu et al. 2005; Pregibon et al. 2007) or surface plasmon resonance (Kanda et al. 2004; Kurita et al. 2006; Psaltis et al. 2006) for signal generation, utilizing electrical detection offers the advantages of simplicity and high sensitivity (Goral et al. 2006; Liao et al. 2006).

Poly(dimethylsiloxane) (PDMS) based microfluidics are most popular (Gijs et al. 2010; McDonald and Whitesides 2002) because the microfabrication of PDMS is easy and inexpensive. The basic microfabrication process of a PDMS based fluidic chip involves patterning of the channel structure, sealing of the open channel, and sensor fabrication (Arora et al. 2010; Dittrich et al. 2006). Typically, a PDMS is used to replicate microchannels using inverse

microfluidic structures from a mold (or master), which can be obtained by photolithography. It is easy to release the PDMS replica from the mold without damaging it or the mold because of its low surface free energy and elasticity. Finally, enclosed microchannels can be obtained by sealing the PDMS replica to a flat surface.

A PDMS can reversibly or irreversibly seal to itself or to other surfaces without distorting its shape (Jo et al. 2000; McDonald et al. 2000). Usually, reversible seals provided by simple Van der Waals contact can not withstand fluid pressures higher than 5 psi (McDonald et al. 2000). When using high viscosity liquids (e.g. human blood or serum, oil) or multi-phase mixtures (e.g. gas-liquid mixture, solid–liquid mixture), a seal between the PDMS and the substrate is required to withstand high pressure that is applied to flow the solution (Thorsen et al. 2001). The oxygen (O_2) plasma treatment becomes necessary to obtain seals that can hold higher pressures. Because O_2 plasma treatment could damage the biosensors, surface modifications are performed after the device assembly of many irreversibly sealed microfluidic biosensor devices, in which the microfluidic channels would be contaminated by the solutions used for surface modification. Hence, it is necessary to prevent damages on the biofunctionalized nanomaterial-based sensors using plasma treatment for the integration of microfluidic devices.

Moreover, controllable functionalization may be obtained if completing the surface modifications before the microfluidic device integration. To achieve this goal without deactivation of the biomolecules immobilized on these nanomaterial-based sensors, methods such as mechanical fixation (Zaytseva et al. 2005) and UV-curable adhesives (McDonald and Whitesides 2002) have been utilized. However, the use of screws in mechanical fixation limits the simplification and miniaturization of microfluidic devices. As a result, assembling a PDMS replica to a pre-functionalized chip *via* irreversible sealing is an important challenge to construct the most effective nanomaterial-based microfluidic biosensors.

Herein, for the first time to our knowledge, we have investigated the use of a low-cost and facile approach that could protect the pre-functionalized biosensor throughout the irreversible sealing process – the use of a shadow mask. Physical masks have been widely applied in microfabrication processes to make patterns on substrates (Egger et al. 2005; Geissler and Xia 2004; Luthi et al. 1999; Schallenberg et al. 2002; Yanagi and Morikawa 1999). In photolithography, optical masks are employed to transfer patterns to photoresists (Geissler and Xia 2004; Rogers et al. 1997). In fact, photoresists are also masks that can be used to transfer patterns onto substrates by preventing underlying materials from being dissolved or removed by etchants (e.g. liquid and plasma etchants) (Hua et al. 2002; Menke et al. 2006; Srituravanich et al. 2004). Furthermore, physical masks are also utilized to prevent self-assembled monolayers (SAMs) being exposed to UV radiation thus the SAMs could not be removed form the protected regions (Ratliff et al. 1999). Inspired by these approaches, we employ a shadow mask for the purpose of preventing damage on functionalized biosensors caused by O_2 plasma treatment. Such a process is similar to reactive ion etching (RIE), but rather than using photoresist, which involves spin coating, UV exposure, and removal steps, the mask introduced in this report is very simple which can be manually placed over the underlying substrate and manually removed after the process. The effects of the shadow mask on the electrical measurement, the fluorescence intensity, and the detection ability of as-prepared and O_2 plasma treated nanowire (NW) biosensors are evaluated in this report. In addition, an integrated microfluidic biosensor device for the detection of Immunoglobulin E (IgE) is demonstrated for a proof-of-principle, which confirms our assumption that the utilization of a shadow mask can protect pre-functionalized biosensors during the plasma treatment.

2 Experimental

2.1 Chemicals

Pyrrole, aniline, NaCl, bovine serum albumin (BSA), 1-ethyl-3-(3-dimethylaminopropyl) carbodiimide (EDC), and N-Hydroxysuccinimde (NHS) were purchased from Sigma Aldrich. 6-carboxyfluorescein (FAM) dye-labeled aptamer (5′-GGGGCACGTTTA- TCCGTCCCTCC TAGTGGCGTGCCCC-3′) was synthesized by Integrated DNA Technologies. IgE was provided by Athens Research & Technology. Goat anti-rabbit immunoglobulin G (IgG, 2 mg/mL, containing 0.1 M NaP, 0.1 M NaCl, and 5 mM azide, pH7.5) antibodies (Abs) and IgG protein (purified rabbit IgG, 5.0 mg/mL, in 10 mM PBS, pH7.4, containing 0.1 % sodium azide) were obtained from Invitrogen. Phosphate buffered saline solution (PBS, 10 mM phosphate, pH7.4) was used to prepare the BSA, IgE, EDC, NHS, and IgG solutions with different concentrations.

2.2 Nanowire preparation and functionalization

Two different kinds of single NWs were fabricated in this work for comparison. One was polypyrrole NWs incorporated with aptamers (aptamer-PPy) during the NWs growth (entrapment), and the other was polyaniline (PANI) NWs that were surface modified by Abs after their growth (covalent binding). These two bio-components (aptamers and antibodies) were used because they are two typical types of receptors in biosensor applications (aptamers are oligonucleic acids, and antibodies are proteins). Details about the

fabrication of the addressable single polymer NW can be found in our previous reports (Hu et al. 2009; Yun et al. 2004). Pre-patterned polymethylmethacrylate (PMMA) nanochannels (about 100 nm in width and 15 um in length) between the electrode pairs (~5 um gap) were used to guide the growth of the NWs while a constant current was applied using a semiconductor analyzer (Agilent B1500A). The growth of the NW was monitored using the potential between the electrode pair. The NW growth was completed when the potential decreased to ~500 μV. There were six groups of Au electrode pairs on one chip. Each group had two electrode pairs. In each group, only one electrode pair was used for NW growth while the other pair acted as a back up pair. Hence, a total number of 6 NWs were grown on one chip. An electrolyte solution consisting of pyrrole monomer (5 mM), NaCl (10 mM) and aptamer (2 μM) was used to prepare the aptamer-PPy NWs. The obtained samples were rinsed with deionized water three times after the preparation of the NWs.

Single PANI NWs were obtained by the same method using an electrolyte solution consisting of aniline monomer (10 mM) and HCl (0.1 M). Surface modifications were performed to immobilize IgG Abs onto the PANI NWs as follows. A mixture solution of EDC/NHS (0.2/0.2 M) with IgG Abs (100 μg/mL) was placed on top of the PANI NWs and incubated at room temperature in a dark room for 3 h. The Abs-immobilized PANI (Abs-PANI) NWs were then rinsed using a PBS solution and deionized water to eliminate any non-immobilized IgG Abs. After the surface modification, the PANI NWs were soaked in a high concentration of BSA (2 mg/mL) for 30 min to block non-specific protein interactions with the NWs.

2.3 Oxygen plasma treatment and microfluidic device integration

A PDMS microfluidic structure with six channels was fabricated through a replica molding process with a SU8 master (silicon elastomer base and curing reagent were mixed in a 10:1 ratio, degassed for 1 h, and then cured at 85 °C for 3 h). While shadow masks can be fabricated and integrated into a device using photolithography (Aljada et al. 2010), in our experiment, the shadow mask is only needed for the O_2 plasma treatment, thus a reusable, simple, and cheap mask was preferred. The mask was machined from an aluminum plate using computer numerical control (CNC) micromachining. The mask had six cantilevers along its top and bottom sides, with each cantilever capable of covering an area with a length of 6.2 mm and a width of 0.8 mm – enough to protect the NW under it (Fig. 1a). Such a design allows the maximum portion of the chip to be exposed to the O_2 plasma without damaging the NWs. The shadow mask was aligned and fixed on top of the silicon chip using stereomicroscopy before the plasma treatment. Figure 1b, c schematically show that the shadow mask can completely cover the NWs. The plasma treatment was performed using plasma cleaner (Harrick PDC-32G) for 1 min (200 mTorr, 18 W). For comparison, several samples were treated with O_2 plasma under the same conditions without the shadow mask.

After the plasma treatment, the shadow mask was quickly removed from the chip and the PDMS replica was then aligned and stacked on the silicon chip to form an irreversible seal. Holes were punched through the PDMS replica on both ends of each microchannel using a 20-gauge needle, and tubings were inserted into the hole to complete the microfluidic device. Typically, the total time for the integration of a microfluidic device was about 10 min. The

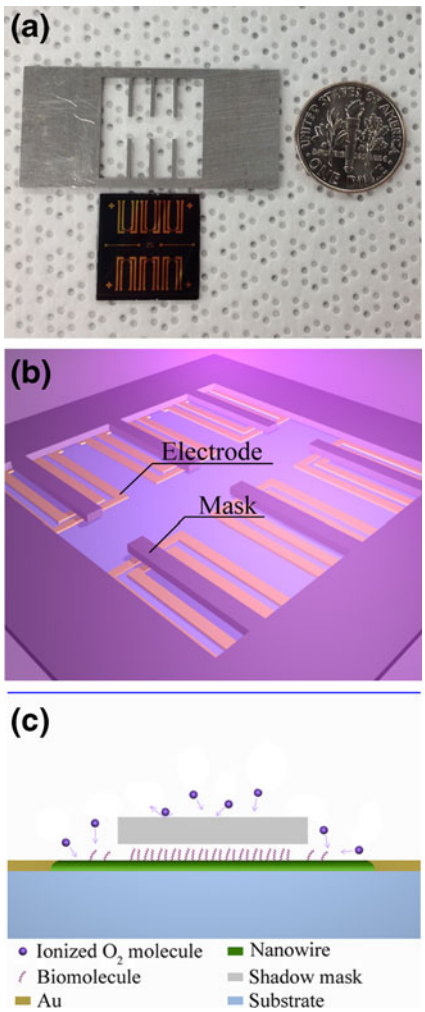

Fig. 1 **a** Photo of an aluminum mask and a chip. The mask has six cantilevers along its top and bottom sides and each cantilever can cover an area with a length of 6.2 mm and a width of 0.8 mm. **b** Schematic illustration of the O_2 plasma treatment of a shadow mask protected chip. **c** Enlarged side view. The bio-functionalized NW is protected by the shadow mask from the plasma. *Arrows* indicate the motions of ionized O_2 molecules

successful injection of fluid into the microfluidic channel through the tubing is shown in Fig. 2.

2.4 Characterizations

To study the protection effects of the shadow mask on the NWs during the plasma treatment, the resistance and fluorescence of both as-prepared and plasma-treated NWs were measured using a semiconductor analyzer and fluorescence microscope (Axioskop, Carl Zeiss). The fluorescence intensities of NW samples were further examined using a microspectrophotometer (CRAIC Technologies) at emission wavelength of 365 nm. All of these measurements were performed at room temperature.

2.5 Protein detection

To determine whether the activity of the biomolecules can be preserved by the shadow mask after plasma treatment, the target protein detection of the as-prepared and plasma treated NWs were compared. Two different biosensors, the aptamer-entrapped PPy NWs and the surface modified PANI NWs, were used for the detection of IgE and IgG respectively. The protein detections were carried out by dividing the NWs into two groups for each case: 1) as-prepared pre-functionalized NWs (Group 1, G-1) and 2) O_2 plasma treated NWs in presence of shadow mask (Group 2, G-2). The conductance of the NWs was monitored by applying a constant current (100 μA) using a semiconductor analyzer. When the conductance of the NW was stabilized in the PBS solution, a droplet of non-specific protein bovine serum albumin (BSA) solution was added, followed by addition of several droplets of target protein solution with different concentrations.

An integrated microfluidic biosensor based on aptamer-PPy NWs was also developed for the detection of IgE protein. The BSA solution was first flowed into the microchannel, followed by several IgE solutions with different concentrations. The same conductance measurement conditions mentioned above were employed.

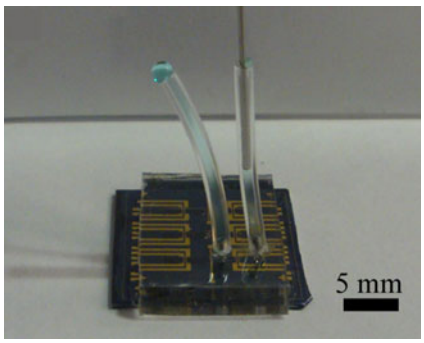

Fig. 2 Demonstration of the microfluidic device integration. It is clear that the fluid can be successfully injected into the microfluidic channel

3 Results and discussion

3.1 Resistance

The *I-V* curves of aptamer-PPy NWs with and without the protection of the shadow mask when treated by O_2 plasma are shown in Fig. 3. The as-prepared NWs measured resistances were about 200 Ω and 320 Ω. The NW which underwent O_2 plasma treatment with no mask showed no current in the *I-V* curve. On the other hand, the resistance of the shadow mask protected NW remained similar (~600 Ω) to its resistance before the plasma treatment. It is well known that plasma has been widely used for surface cleaning, in which process energetic ionized gas molecules are used to break organic bonds and remove organic contaminates. Therefore, without any protection, it is easy to create breaks on NWs with O_2 plasma. These breaks can be prevented *via* the use of a shadow mask, which is confirmed by the results demonstrated above. Conducting polymers are very sensitive to humidity changes, and many conducting polymers based humidity sensors have been reported (Jain et al. 2003; Parvatikar et al. 2006). Therefore, the resistance increase observed in the NW protected by the shadow mask is believed to have resulted from the low humidity in the vacuum during the plasma treatment.

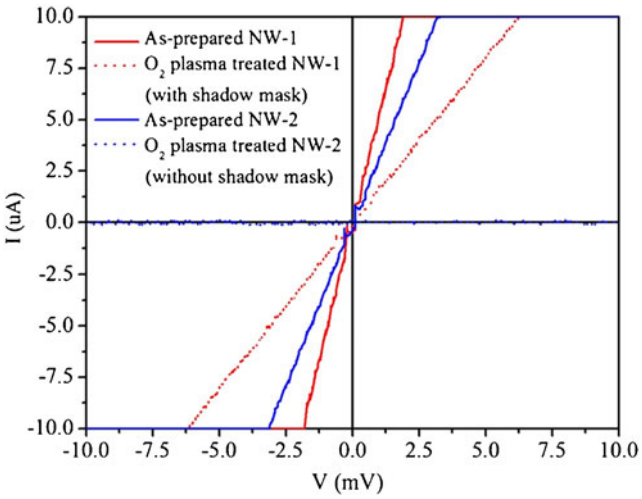

Fig. 3 *I-V* curves of aptamer-PPy NWs before (*solid lines*) and after (*dash lines*) the plasma treatment with (*red*) and without (*blue*) the use of shadow mask

3.2 Fluorescence

Fluorescence images of the NWs functionalized with fluorescently labeled biomolecules were taken using fluorescence microscopy, as shown in Fig. 4a. To some extent, the damage on the NWs caused by plasma treatment can be represented by their fluorescence intensity changes. It can be observed from the images that, in the absence of the shadow mask, a clear bright line (aptamer-PPy NW) was broken into two short lines with reduced fluorescence intensity after the plasma treatment. Conversely, in the presence of shadow mask, the NW showed non-appreciable changes in fluorescence intensity after the plasma treatment. Quantitative characterization on the fluorescence of the NWs was further performed using a microspectrophotometer. The results are shown in Fig. 4b. The significant reduction in fluorescence intensity of the unprotected NW indicates that plasma treatment can indeed easily damage the NW and the biomolecules. In contrast, the small intensity reduction observed for the shadow mask NW indicates the protective effectiveness of the shadow mask.

3.3 IgE and IgG protein detection without microfluidic device

In order to determine whether the bioactivity of the biomolecules on individual NWs can be preserved by using a shadow mask during the plasma treatment, protein detections were carried out with aptamer-PPy NWs and Abs-PANI NWs respectively. Each type of NWs contained two groups – functionalized NWs before plasma treatment (as-prepared NWs, G-1) and shadow mask protected samples treated with O_2 plasma (G-2). Bioactivity results for these groups were compared. IgE detection using aptamer-PPy NWs (Fig. 5a) showed that the response changes in the NWs in G-2 decreased a little compared to the NWs in G-1. The average of the normalized conductance decreases from G-1 to G-2 for different IgE concentrations from 0.1 to 1,000 nM was ~0.42 % with a standard deviation of 0.16 %. Nevertheless, the measured values of G-2 remain within the distinguishable level for IgE detection. In the case of IgG detection for Abs-modified PANI NWs, the same phenomenon was observed except at high IgG concentrations (Fig. 5b). The large error bars were due to the variation in some synthesized nanowires. Nevertheless, a trend of conductance change increase with increase in concentration can be observed. An insufficient concentration of active Abs on the PANI NWs could be the main reason for the decreased sensitivity in high IgG concentrations. Antibodies are very sensitive to environmental changes, thus in the absence of protectants (e.g. sucrose), they could become dehydrated in a dry environment created by a vacuum condition, resulting in a loss of biological activity upon rehydration (Allison et al. 1998). Relatively higher chamber pressures may be a solution to improve the performance of Abs-PANI NWs (e.g. use atmospheric-pressure O_2 plasma) (Da Ponte et al. 2011; Kamel et al. 2011; Xie et al. 2011). In either case, this result still shows that the shadow mask plays an important protective role in preserving the bioactivity of Abs-PANI NWs. Specifically, the shadow mask can preserve the bioactivity of functionalized single NW which has undergone the O_2 plasma treatment.

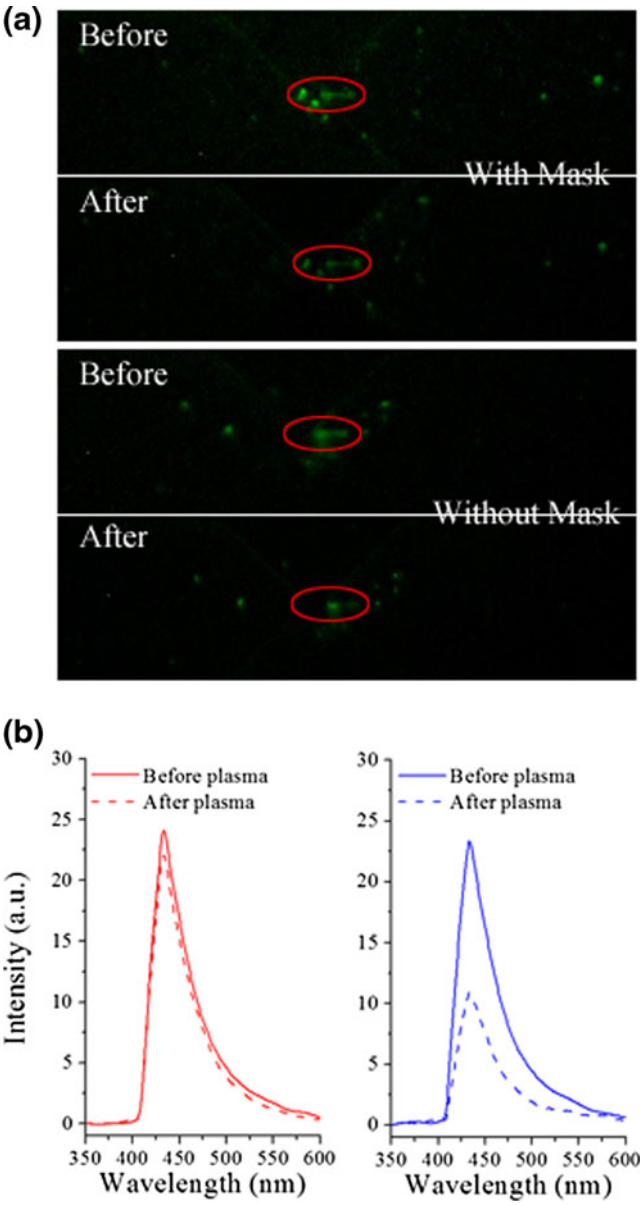

Fig. 4 Fluorescence characterizations of the NWs. **a** Fluorescence images of aptamer-PPy NWs before and after the plasma treatment with and without the use of shadow mask. **b** The fluorescence intensity of samples before (*solid line*) and after (*dash line*) plasma treatment with (*red*) and without (*blue*) the use of shadow mask

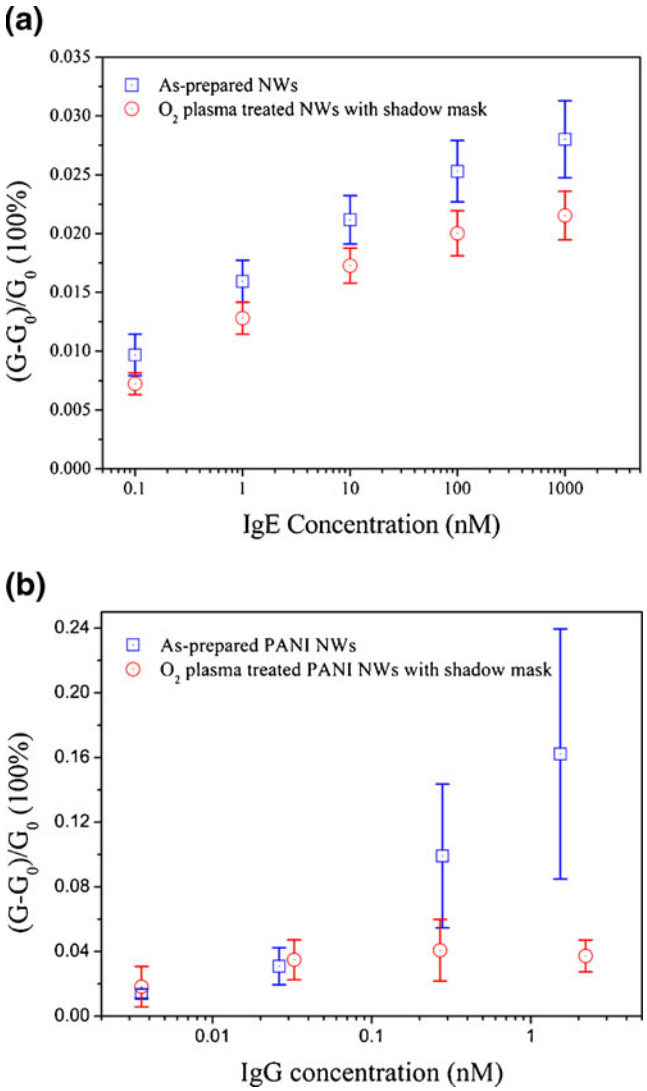

Fig. 5 Comparison of biofunctionalized NWs before plasma treatment (G-1) and after plasma treatment with the protection of shadow mask (G-2). **a** IgE detection responses from two groups of aptamer-PPy NWs. **b** IgG detection responses from two groups of Abs-PANI NWs. G_0 is the stabilized conductance of the NWs upon addition of PBS solution, and G is the stabilized conductance of the NWs upon addition of target solutions (IgE or IgG) with different concentrations. The average of normalized response changes and *error bar* were calculated from three different NWs for each protein concentration

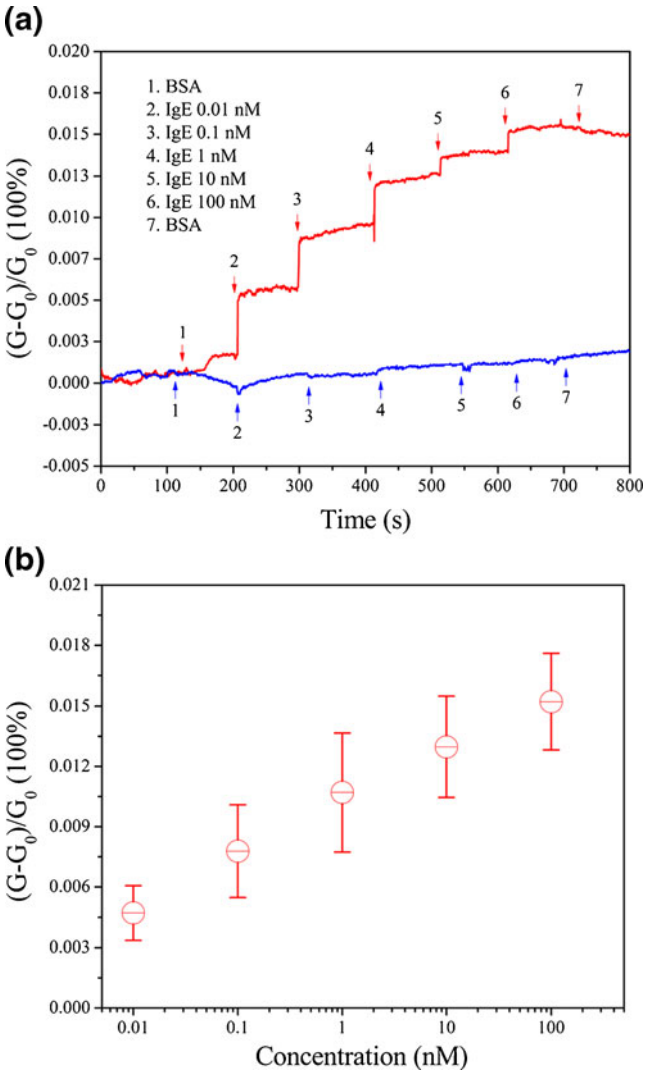

Fig. 6 IgE detections using aptamer-PPy single NWs based microfluidic biosensors. **a** Normalized real-time response of microfluidic biosensor (*red*) and PPy NW (*blue*) to BSA and IgE solutions. Arrows indicate the points of injecting protein solution. **b** Normalized conductance changes of the microfluidic biosensors as a function of IgE concentration

3.4 Microfluidic biosensor for IgE detection

Previous results show that the O_2 plasma treatment has a greater impact on antibody modified PANI NWs; therefore only aptamer-PPy NWs were integrated into the microfluidic biosensor device. As shown in Fig. 6a, a stepwise response was observed upon the injection of IgE solutions into the microchannel. As the IgE concentration increased from 0.01 to 100 nM, the conductance changes of this microfluidic biosensor consistently increased from 0.58 % to 1.56 %. Remarkably, the response and stabilization times for this microfluidic biosensor were very fast (a few seconds), which is desirable for biosensors. Moreover, the slight changes in the negative control of PPy NW corresponding to BSA and IgE solutions indicate an excellent specificity for this microfluidic biosensor.

The sensitivity of this microfluidic biosensor was calculated using three biosensors. Results are shown in Fig. 6b. A dynamic range from 0.01 nM (2 ng/ml) to 100 nM (20 μg/mL) was obtained. This type of microfluidic biosensor showed high sensitivity, with a ~0.5 % change in conductance at the lowest IgE concentration of 0.01 nM (2 ng/mL). These results demonstrate the applicability of this microfluidic biosensor to detect IgE concentrations below and above 1.2 nM (240 ng/mL), which has been

established as the normal level of IgE in non-allergic adults (Cole et al. 2007; Kim et al. 2009).

4 Conclusions

We have successfully demonstrated that employing a shadow mask protects pre-functionalized NWs during O_2 plasma treatment and enables the integration of irreversibly sealed microfluidic devices. Significant differences were observed between the bio-functionalized nanowire sensors treated with O_2 plasma with and without using a shadow mask. In the absence of a shadow mask, NWs are destroyed after plasma treatment, as shown by the increase in resistance and decrease in fluorescence intensity. On the other hand, NWs with the shadow mask were protected, maintaining a low resistance and high fluorescence intensity post plasma treatment. The detection of proteins by aptamer-PPy and Abs-PANI NWs further demonstrated that the shadow mask can preserve the bioactivity of the immobilized biomolecules and that a microfluidic biosensor can be fabricated after the plasma treatment. The integrated microfluidic biosensor developed in this work exhibited fast response and rapid stabilization times. This simple but novel approach provides a significantly easy way to assemble irreversibly sealed nanomaterial-based microfluidic devices without deactivating the pre-functionalized detection elements. Therefore this technique can be widely applied to nanomaterial-based microfluidics for the purposes of biomolecule detection and clinical diagnostics.

Acknowledgments This research is supported by National Science Foundation (NSF) ECCS 0824035 and National Institute of Health (NIH) 1R21B008825 and Mascaro Center of Sustainable Innovation (MCSI). Minhee Yun would like to acknowledge the Korea Brain Pool program.

References

M. Aljada, K. Mutkins, G. Vamvounis, P. Burn, P. Meredith, J. Micromech. Microeng. **20**(7), 6 (2010)
S.D. Allison, T.W. Randolph, M.C. Manning, K. Middleton, A. Davis, J.F. Carpenter, Arch. Biochem. Biophys. **358**(1), 171–181 (1998)
A. Arora, G. Simone, G.B. Salieb-Beugelaar, J.T. Kim, A. Manz, Anal. Chem. **82**(12), 4830–4847 (2010)
A. Bange, H.B. Halsall, W.R. Heineman, Biosens. Bioelectron. **20**(12), 2488–2503 (2005)
E.Y. Chan, N.M. Goncalves, R.A. Haeusler, A.J. Hatch, J.W. Larson, A.M. Maletta, G.R. Yantz, E.D. Carstea, M. Fuchs, G.G. Wong, S.R. Gullans, R. Gilmanshin, Genome Res. **14**(6), 1137–1146 (2004)
J.R. Cole, L.W. Dick, E.J. Morgan, L.B. McGown, Anal. Chem. **79**(1), 273–279 (2007)
G. Da Ponte, E. Sardella, F. Fanelli, R. d'Agostino, P. Favia, Eur. Phys. J. Appl. Phys. **56**(2), 4 (2011)
P.S. Dittrich, K. Tachikawa, A. Manz, Anal. Chem. **78**(12), 3887–3907 (2006)
S. Egger, A. Ilie, Y.T. Fu, J. Chongsathien, D.J. Kang, M.E. Welland, Nano Lett. **5**(1), 15–20 (2005)
M. Geissler, Y.N. Xia, Adv. Mater. **16**(15), 1249–1269 (2004)
M.A.M. Gijs, F. Lacharme, U. Lehmann, Chem. Rev. **110**(3), 1518–1563 (2010)
V.N. Goral, N.V. Zaytseva, A.J. Baeumner, Lab Chip **6**(3), 414–421 (2006)
Y. Hu, A.C. To, M. Yun, Nanotechnology **20**(28), 8 (2009)
F. Hua, J. Shi, Y. Lvov, T. Cui, Nano Lett. **2**(11), 1219–1222 (2002)
S. Jain, S. Chakane, A.B. Samui, V.N. Krishnamurthy, S.V. Bhoraskar, Sensors Actuators B Chem. **96**(1–2), 124–129 (2003)
B.H. Jo, L.M. Van Lerberghe, K.M. Motsegood, D.J. Beebe, J. Microelectromech. Syst. **9**(1), 76–81 (2000)
M.M. Kamel, M.M. El Zawahry, H. Helmy, M.A. Eid, J. Text. Inst. **102**(3), 220–231 (2011)
V. Kanda, J.K. Kariuki, D.J. Harrison, M.T. McDermott, Anal. Chem. **76**(24), 7257–7262 (2004)
Y.H. Kim, J.P. Kim, S.J. Han, S.J. Sim, Sensors Actuators B Chem. **139**(2), 471–475 (2009)
R. Kurita, Y. Yokota, Y. Sato, F. Mizutani, O. Niwa, Anal. Chem. **78**(15), 5525–5531 (2006)
S. Kwakye, A. Baeumner, Anal. Bioanal. Chem. **376**(7), 1062–1068 (2003)
W.Y. Liao, C.H. Weng, G.B. Lee, T.C. Chou, Lab Chip **6**(10), 1362–1368 (2006)
W.T. Liu, L. Zhu, Q.W. Qin, Q. Zhang, H.H. Feng, S. Ang, Lab Chip **5**(11), 1327–1330 (2005)
R. Luthi, R.R. Schlittler, J. Brugger, P. Vettiger, M.E. Welland, J.K. Gimzewski, Appl. Phys. Lett. **75**(9), 1314–1316 (1999)
J.C. McDonald, G.M. Whitesides, Acc. Chem. Res. **35**(7), 491–499 (2002)
J.C. McDonald, D.C. Duffy, J.R. Anderson, D.T. Chiu, H.K. Wu, O.J.A. Schueller, G.M. Whitesides, Electrophoresis **21**(1), 27–40 (2000)
E.J. Menke, M.A. Thompson, C. Xiang, L.C. Yang, R.M. Penner, Nat. Mater. **5**(11), 914–919 (2006)
N. Parvatikar, S. Jain, S. Khasim, M. Revansiddappa, S.V. Bhoraskar, M. Prasad, Sensors Actuators B Chem. **114**(2), 599–603 (2006)
D.C. Pregibon, M. Toner, P.S. Doyle, Science **315**(5817), 1393–1396 (2007)
D. Psaltis, S.R. Quake, C.H. Yang, Nature **442**(7101), 381–386 (2006)
L.P. Ratliff, R. Minniti, A. Bard, E.W. Bell, J.D. Gillaspy, D. Parks, A.J. Black, G.M. Whitesides, Appl. Phys. Lett. **75**(4), 590–592 (1999)
J.A. Rogers, K.E. Paul, R.J. Jackman, G.M. Whitesides, Appl. Phys. Lett. **70**(20), 2658–2660 (1997)
T. Schallenberg, C. Schumacher, S. Gundel, W. Faschinger, Thin Solid Films **412**(1–2), 24–29 (2002)
S.A. Soper, K. Brown, A. Ellington, B. Frazier, G. Garcia-Manero, V. Gau, S.I. Gutman, D.F. Hayes, B. Korte, J.L. Landers, D. Larson, F. Ligler, A. Majumdar, M. Mascini, D. Nolte, Z. Rosenzweig, J. Wang, D. Wilson, Biosens. Bioelectron. **21**(10), 1932–1942 (2006)
W. Srituravanich, N. Fang, C. Sun, Q. Luo, X. Zhang, Nano Lett. **4**(6), 1085–1088 (2004)
T. Thorsen, R.W. Roberts, F.H. Arnold, S.R. Quake, Phys. Rev. Lett. **86**(18), 4163–4166 (2001)
J.F. Xie, D.W. Xin, H.Y. Cao, C.T. Wang, Y. Zhao, L. Yao, F. Ji, Y.P. Qiu, Surf. Coat. Technol. **206**(2–3), 191–201 (2011)
H. Yanagi, T. Morikawa, Appl. Phys. Lett. **75**(2), 187–189 (1999)
M. Yun, N.V. Myung, R.P. Vasquez, C. Lee, E. Menke, R.M. Penner, Nano Lett. **4**, 419–422 (2004)
N.V. Zaytseva, V.N. Goral, R.A. Montagna, A.J. Baeumner, Lab Chip **5**(8), 805–811 (2005)